ACS OMEGA

http://pubs.acs.org/journal/acsodf

Article

Innovative Codeposition of a Ag−Al_2O_3 Layer: An Attractive Combination of High Durability and Lack of Cytotoxicity for Public Space Applications

Massimo Calovi,* Stefania Meschini, Maria Condello, and Stefano Rossi

Cite This: https://doi.org/10.1021/acsomega.2c02872

Read Online

ACCESS | Metrics & More | Article Recommendations

ABSTRACT: Today, the use of silver in surfaces for public environments is very frequent, as it ensures high antimicrobial activities, avoiding the continuous disinfection of the surfaces themselves. Similarly, thanks to its interesting combination of technological properties, anodized aluminum is widely employed in the production of components for applications in public spaces. Therefore, this work describes a simple method of the codeposition of silver and anodized aluminum to combine the remarkable properties of Al_2O_3 layers with the antibacterial performances of silver. The effect of silver in modifying the durability features of the anodized aluminum layer was evaluated by means of various accelerated degradation techniques, such as the exposure in a climatic chamber to UV-B radiation or an aggressive atmosphere simulated by the Kesternich test. These analyses showed the good compatibility between Ag and the alumina matrix, whose durability performances were not particularly influenced by silver. Furthermore, the composite layers did not express relevant cytotoxicity activity, as evidenced by Trypan blue flow cytometry analysis and microscopy observations, ensuring the possible use of this material in applications in close contact with humans. This same conclusion was reached by observing an almost negligible ionic release of Ag by the composite layers, even following severe degradation of the alumina matrix due to exposure to a particular acid solution. In conclusion, this work presents an innovative material that can be used in public spaces, thanks to its interesting combination of high durability and low cytotoxicity.

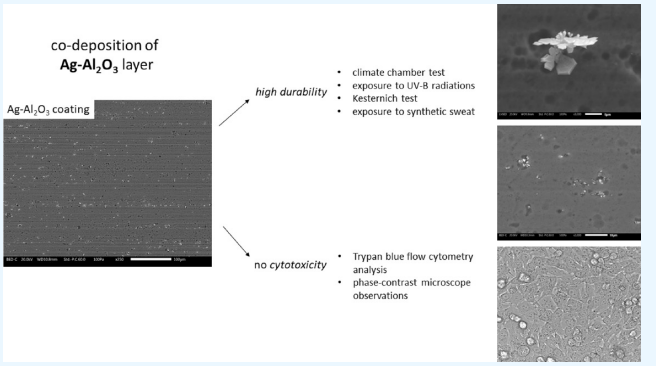

1. INTRODUCTION

One of the most delicate current industrial challenges lies in the production and use of multifunctional surfaces, which are capable of associating high levels of durability with other useful features. The SARS-CoV-2 pandemic has highlighted the need to focus attention on the effect such surfaces can have on people's health. Specifically, today, a lot of effort has been oriented to the production of materials and surfaces that can limit the growth and proliferation of micro-organisms.[1] Surfaces, in fact, especially in public environments, represent one of the main means for the transmission of pathogens.[2]

The simplest solution adopted during this pandemic was the continuous sanitation and disinfection of the surfaces to counteract the spread of the virus. However, this option immediately showed some critical issues, mainly linked to the significant efforts, in terms of economy and time, to implement continuous disinfection of surfaces in public spaces, whose performance and effectiveness are, among other things, dependent on the degree of use of the surfaces themselves.[3] Furthermore, the frequent use of aggressive disinfectants can lead to the modification of both the aesthetic perceptive and functional properties of the surfaces. The aspect of the surface contamination highlighted with the SARS Cov2 emergency is not limited to this virus. In fact, this problem has always been present, especially in hospitals and communities, in particular, for resistant antibiotic bacteria. Consequently, the academic research field has directed its resources to study innovative surfaces that do not require continuous disinfection, but that are able to act directly on the proliferation of viruses and bacteria, limiting it. This preventive approach, in addition to reducing the use of disinfectants, seems to represent the most concrete solution in fighting the indirect spread and transmission of pathogenic micro-organisms through surfaces.

Aluminum is one of the most used materials for the construction of surfaces and components in public spaces,[4−6] thanks to an interesting combination of technological properties, such as high specific strength, thermal conductivity, workability, low density, low cost, and pleasant appearance. To

Received: May 9, 2022
Accepted: June 30, 2022

overcome the obvious lack of durability,[7,8] aluminum surfaces are usually subjected to the anodizing process,[9−12] which improves the protective performance of the component,[13,14] its chemical resistance,[15,16] and aesthetic features over time.[17,18] Hence, to produce inherently antimicrobial surfaces, anodized aluminum has recently been the subject of several implementation studies.[19−21]

In recent years, silver has proved to exert a strong biocidal effect, acting as an effective antimicrobial agent even at very low concentrations.[22−26] Adhering to the cell wall and modifying its permeability, deactivating respiratory enzymes, and hindering DNA replication,[27] silver is responsible for a high antibacterial activity. Consequently, following the SARS-CoV-2 pandemic, silver and silver oxide have been extensively studied, assessing their antimicrobial features,[28] studying the cytotoxicity activities,[29] and evidencing bioactive properties.[30] Thus, these aspects make silver the ideal candidate for the creation of anodized aluminum layers with antibacterial performance.

The literature offers the first work in which the anodized aluminum has been reinforced with silver already 20 years ago, by means of an electrodeposition process, providing the surface with innovative antibacterial performances.[31] This work represented a point of reference for several subsequent studies, which have tried to deposit silver on the anodized aluminum surface by exploiting different techniques, such as the electroless deposition method,[32−34] the hydrothermal deposition process,[35] the photoreduction deposition method,[35] or a simple process of codeposition of silver powder with alumina during the anodizing step.[36] The latter method seems to be the most encouraging, as the recent work has highlighted the excellent bactericidal performance of the surfaces obtained by codeposition with silver nitrate.[37]

However, once the antibacterial features of silver have been widely confirmed, scholars are wondering what are the consequences of its addition to the surfaces of public spaces on people's health in terms of levels of cytotoxicity. It is known that one of the causes of bacterial death is that silver nanoparticles are able to enter the bacterial wall and alter the cell membrane, inducing oxidative stress resulting in damage to proteins and the respiratory mitochondrial chain, as well as at the replicative level.[38] There are many works in the literature that indicate the toxicity induced by the release of silver ions even in aquatic organisms for the osmotic imbalance caused at the level of ATPase-Na+ K+ by the ions themselves.[39] Silver particles were also detected in the stratum corneum and in the deep layer of the epidermis even after 5 days of exposure.[40]

Therefore, it is important to evaluate both the possible alterations of the surface of silver anodized aluminum that could lead to nanomaterials and ion release and its correlation with possible toxicity in the human epidermis.

Thus, this work focuses on the characterization of the durability behavior of silver-containing anodized aluminum surfaces, whose bactericidal performances have already been assessed.[37] In detail, the surfaces of aluminum oxide layers were exposed to aggressive environments, with particular thermal changes, UV radiation, and sulfur dioxide atmosphere, evaluating the effect introduced by silver in modifying their durability. Thus, the release of silver ions was assessed by placing the samples in contact with a lactic acid solution simulating human sweat. To evaluate the possible toxicity induced by contact with the surfaces, cytotoxicity resulting from continuous exposure of normal and pathological human cells to anodized aluminum surfaces with and without silver was studied. The presence of silver ion release in the medium in which the cells were seeded simultaneously with the aluminum samples, anodized aluminum, silver content in anodized aluminum at a low concentration (A) and a high concentration (B) was also evaluated. In vitro toxicity assays were performed by quantitative colorimetric analysis of Trypan blue provided by flow cytometry. Morphological analysis was performed by light microscopy on all samples from two human cell lines, a human melanoma line simulating a possible precancerous pathological situation present on the skin surface and a human fibroblast line obtained from an explant of a patient.

2. EXPERIMENTAL SECTION

2.1. Materials. A 6082 aluminum alloy (Si 0.7−1.3 wt %, Mg 0.6−1.2 wt %, Mn 0.4−1.0 wt %; Al bal.) was purchased from Metal Center S.R.L. (Trento, Italy). Sulfuric acid, silver nitrate, nitric acid, sodium hydroxide, sodium meta bisulfate, sulfamic acid, and lactic acid were purchased from Sigma-Aldrich and used as received. The human fibroblast (HF) was obtained from the Molecular and Cell Biology Laboratory of IDI Hospital (Rome, Italy) by a human explant after abdominoplasty surgery. The human fibroblasts were grown in Dulbecco's modified Eagle's medium (DMEM) with high glucose, supplemented with 10% foetal bovine serum (FBS) and 1% penicillin (50 U/mL)—streptomycin (50 μg/mL). The immortalized human melanoma line (A375) was purchased from American Type Culture Collection (ATCC) and was cultured in RPMI 10% FBS, 1% penicillin (50 U/mL)−streptomycin (50 μg/mL), and 1% nonessential amino acids in a humidified atmosphere of 5% CO_2 in a water-jacketed incubator at 37 °C.

2.2. Composite Layer Production by Codeposition with Silver Nitrate. The addition of silver in the aluminum oxide layer was achieved by a single-step codeposition process. The samples were realized following a procedure described in a previous study,[37] introducing the silver nitrate directly into a sulfuric acid anodization bath. First, the aluminum plates (80 mm × 60 mm × 2 mm dimensions) were subjected to a pretreatment process, consisting of an etching step of 300 s in 5 wt % NaOH solution, followed by a 30 s desmutting step in 10% v/v HNO_3. Subsequently, the samples were placed in the sulfuric acid bath and anodized at 20 V at a temperature of 20 ± 1 °C for 20 min. Finally, the aluminum-based plates were properly rinsed with distilled water and sealed by soaking in boiled water (96 °C for 20 min).

To study the effect of silver concentration on the performance of the composite layer, three different samples were produced, modifying the sulfuric acid bath, as described in Table 1. The 20 wt % H_2SO_4 bath was used for the deposition of the reference sample called X. Thus, 0.85 and 1.70 g/L $AgNO_3$ were added in the H_2SO_4 bath to realize the two series of composite samples labeled as A and B,

Table 1. Samples' Nomenclature with Relative $AgNO_3$ Amount Added to the H_2SO_4 Anodization Bath

anodization bath	$AgNO_3$ addition [g/L]	sample nomenclature
20 wt % H_2SO_4	0.00	X
	0.85	A
	1.70	B

https://doi.org/10.1021/acsomega.2c02872
ACS Omega XXXX, XXX, XXX−XXX

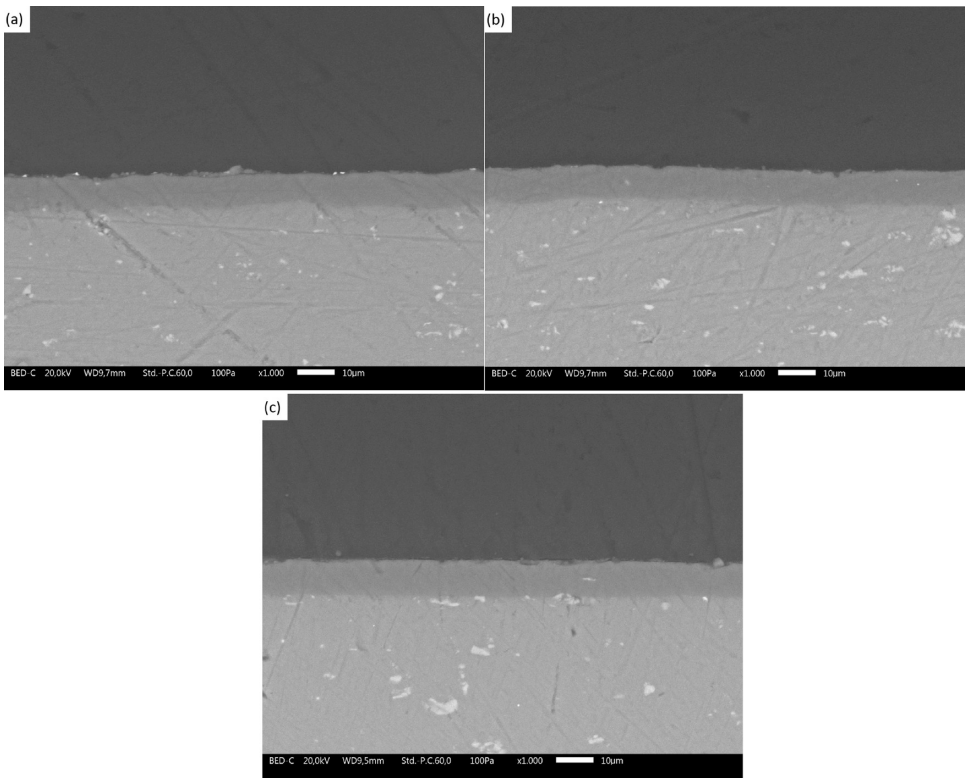

Figure 1. SEM micrographs of the cross section of sample X (a), sample A (b), and sample B (c), respectively.

respectively. These two modified H_2SO_4 baths were stirred for 30 min before the anodization step to favor the homogeneous dispersion of the silver nitrate powder.

Despite the residual amount of silver nitrate added to the anodizing bath, the implementation of the manufacturing process of samples A and B caused a non-negligible increase in production costs. In fact, the high value of silver nitrate, compared to that of sulfuric acid, leads to an increase in expenses of 29 and 58% for the deposition of samples A and B, respectively. Such an increase in production costs must be justified by a net improvement in the performance of the product, as it is subsequently demonstrated by the various characterization tests. However, it must be considered that the success of the anodizing process also relies in its cost-effectiveness. Definitely, the percentage increase in spending due to silver nitrate can be easily supported by the manufacturing companies.

2.3. Characterization. The samples were analyzed by a low vacuum scanning electron microscopy (SEM JEOL IT 300) observation, both in top-view and in cross section, to assess if the addition of silver nitrate affects the yield of the anodizing process, modifying the surface morphology of the composite layers. These studies were implemented by energy-dispersive X-ray spectroscopy (Bruker Quantax EDXS) analysis and carried out to map the silver powder distribution in the aluminum oxide layer.

To evaluate the durability of the samples, considering their possible application in outdoor environments, the three series of plates were subjected to various accelerated degradation tests, simulating exposures in aggressive environments. First of all, the samples were subjected to a climatic chamber exposure, undergoing continuous thermal changes. The test consisted of a succession of cycles of 6 h at a temperature of 40 °C and relative humidity > 90%, followed by 6 h at a temperature of −5 °C. The samples were monitored after 1, 3, and 7 days of exposure in the climatic chamber through an optical stereoscopy (Nikon SMZ25) and electronic microscopy observation, evaluating the possible influence of silver in limiting the durability of the alumina layer.

To study the behavior of the composite layers exposed to sunlight, the samples were tested in a UV-B chamber (313 nm) for 7 days, employing a UV173 Box Co.Fo.Me.Gra, following the ASTM G154-16 standard.[41] The effect of UV-B radiation was evaluated by observing the samples using a scanning electron microscope at the end of the test. Finally, the samples were studied with the Kesternich test, following the ASTM G87 standard,[42] simulating an industrial atmosphere. The analysis consisted of seven cycles lasting 24 h each, made of 8 h with the chamber rich in sulfur dioxide at a temperature of 40 °C and subsequent 16 h with continuous air blowing for the chamber cleaning. The damage caused by the particularly aggressive atmosphere toward the surface of the samples was evaluated by microscopic observations after the first, third, and seventh cycles.

A previous work[37] has highlighted the degradation these surfaces undergo in contact with a solution-simulating human sweat. In this study, the authors focused on evaluating the silver ion release values by the composite layer exposed to this solution to assess the level of danger of multiple or prolonged contact of the samples with human skin. Thus, the samples were immersed for 28 days in a particular acid solution at a temperature of 60 °C, taking as a reference the ISO 12870:2016 standard (section 8.5)[43] for the perspiration resistance. The standard has been modified, using a 50 g/L lactic acid solution, free of sodium chlorides: the reaction between silver and sodium chloride, with consequent deposition of silver chlorides, in fact, would have falsified the ionic release test. The release of silver ions was evaluated

https://doi.org/10.1021/acsomega.2c02872
ACS Omega XXXX, XXX, XXX−XXX

during the 28 days' test and measured by inductively coupled plasma (ICP; Spectro-Ciros).

Both cell lines were used to assess cytotoxicity by the Trypan blue (TB) exclusion assay. The cells were maintained as a monolayer culture in T75 cm^2 tissue culture flasks at a controlled condition of 37 °C in a humidified atmosphere containing 5% CO_2 in an incubator. When cells reached 70−80% confluent monolayer, cells were enzymatically detached with a trypsin−EDTA solution and were passaged into a 6 cm diameter Petri dish for control cells and plaque plus cells. After 24, 48, and 72 h from seeding, the plaques were removed; the cells were detached and rinsed with PBS solution. After incubation with TB solution, defined as the optimum concentration for distinguishing unstained living cells from fluorescent dead cells, cells were analyzed by a BDLSRII flow cytometer (Becton, Dickinson & Co., Franklin Lakes, NJ) equipped with a 15 mW, 488 nm, air-cooled argon-ion laser and a Kimmon HeCd 325 nm laser. The TB fluorescence emission was collected through a 670 nm band pass filter. At least 10,000 events are acquired in log mode. The percentage of TB-positive cells was calculated by FACS Diva software (Becton, Dickinson & Company). The morphology of the samples was investigated by an ECLIPSE Ti2 light microscope (Nikon Europe, Amsterdam, Netherlands). The results obtained from three independent experiments were expressed as mean ± standard deviation (SD). One-way analysis of variance (ANOVA) and Dunnett post hoc analysis were applied to reveal differences between all treated and control samples using GraphPad Prism 5 software (GraphPad, San Diego, CA).

3. RESULTS AND DISCUSSION

3.1. Coating Morphology. The three series of samples were observed by a scanning electron microscope (SEM) to verify possible defects introduced by the addition of silver nitrate in the sulfuric acid bath. Figure 1 shows the cross sections of the three layers, which appear compact, continuous, and free from obvious defects. Thus, the modification of the sulfuric acid bath with silver nitrate does not seem to have altered the anodization process yield.

Similarly, the three different aluminum oxide layers possess a comparable thickness of about 12 μm. Table 2 summarizes the thickness values of the three layers, obtained from 50 measurements per sample series.

Table 2. Thickness of the Three Sample Series

sample	layer thickness [μm]
X	12.1 ± 0.9
A	12.7 ± 0.8
B	12.6 ± 0.4

Definitely, silver nitrate, which is easily dissolved in the sulfuric acid bath, does not influence the growth of the aluminum oxide layer. This result was already observed in a previous literature work,[37] which studied in depth the silver deposition process during the anodization, that occurs by self-reduction in proximity to interstitial elements, such as silicon and manganese, present in the aluminum alloy. Figure 2 reveals this phenomenon: silicon and manganese counteract the growth of the oxide layer but at the same time favor the reduction of silver, which is trapped in the cavities of the Al_2O_3 film. These cavities and, consequently, the silver traces possess dimensions ranging from 2 to 7 μm.

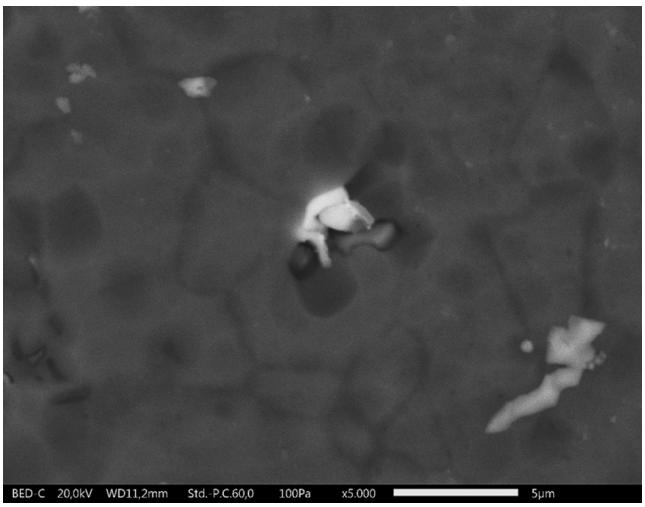

Figure 2. SEM observation of silver powder reduced in the Al_2O_3 layer of sample A.

Thus, the reduction of silver and its distribution on the surface of the samples strongly depends on the presence of the interstitial elements in the aluminum alloy. From Figure 3, representative of the surface of sample B observed with an SEM, several clear points distinguishable from the matrix can be appreciated. These clear signals are actually silver powders, as confirmed by the relative EDXS map of the Ag element, on the right of the figure. The EDXS map highlights an important characteristic, namely, the homogeneous distribution of traces of silver in the alumina layer, which is a fundamental aspect for the antimicrobial action of the surface. The same aspect is perceived on both the surface of sample A and sample B, with different silver concentrations detected, equal to 0.58 ± 0.06 and 1.15 ± 0.07 wt %, respectively. Thus, the ratio of the amount of silver nitrate added to the anodizing bath, between sample A and sample B, is reflected in the concentration of silver analyzed in the composite Al_2O_3−Ag layers.

3.2. Sample Exposure to Different Aggressive Environments. The three series of samples were subjected to different accelerated degradation tests, evaluating the effect introduced by silver in modifying the durability performance of the alumina matrix. Since anodized aluminum is often employed in public outdoor environments, the behavior of the samples was assessed by exposing them to particular thermal changes, UV-B radiation, and aggressive atmospheres.

3.2.1. Climate Chamber Test. The thermal stability of the samples was evaluated by 7 days' exposure in a climatic chamber. The work of Wang et al.[44] describes in depth the degradation phenomena of silver, highlighting how deterioration of Ag nanostructures and films is closely linked to the presence of surface-adsorbed water. Therefore, to further stress the samples, the cycles at a temperature of 40 °C were performed at relative humidity higher than 90%. On the other hand, the temperature range between 40 and −5 °C was carried out to simulate environments subject to strong temperature variations.

The samples were monitored after 1, 3, and 7 days to observe a possible degradation of the composite layers. However, the three series of samples evidenced no appreciable defectiveness and degradation phenomena. The images of

https://doi.org/10.1021/acsomega.2c02872
ACS Omega XXXX, XXX, XXX−XXX

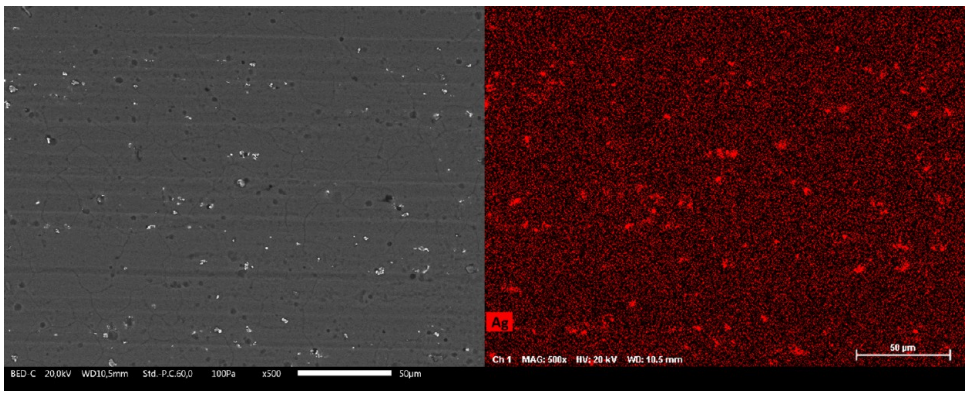

Figure 3. SEM micrographs of the surface of sample B, with the corresponding EDXS map of the Ag element distribution.

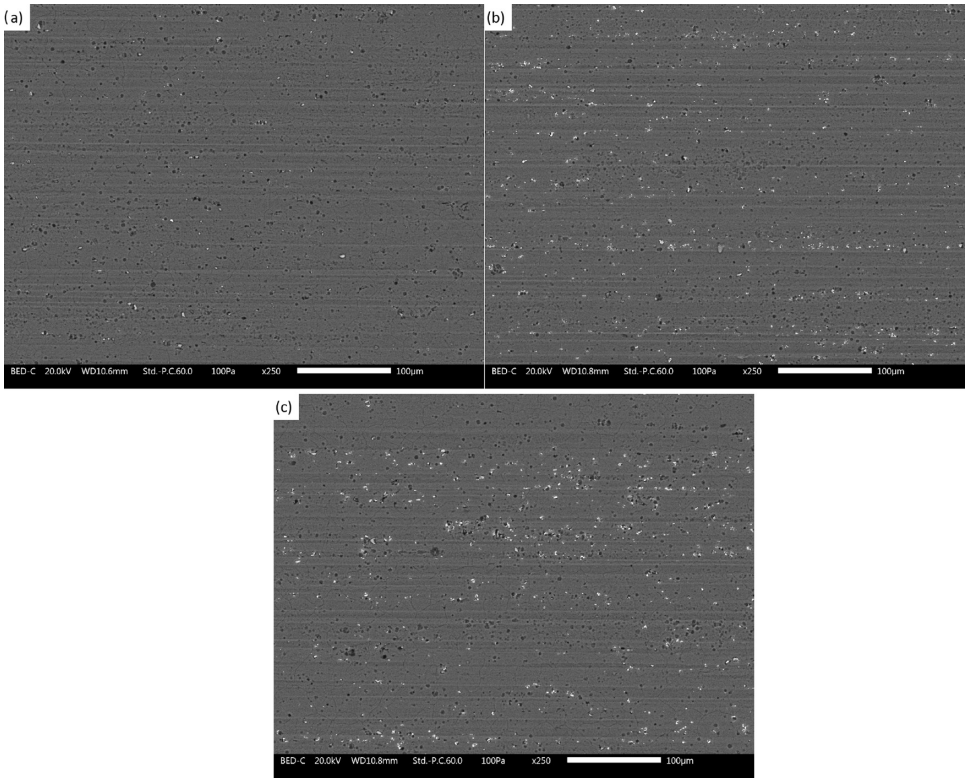

Figure 4. SEM micrographs of the surface of sample X (a), sample A (b), and sample B (c), respectively, after 7 days of exposure in the climate chamber.

Figure 4, acquired by SEM after 7 days of testing, show the surface morphology of the three series of coatings. The alumina layer of sample X (Figure 4a) exhibits the typical morphology of anodized aluminum coatings, with some porosity due to the presence of silicon and manganese in the 6082 aluminum alloy. At the end of the test, no cracks or defects were appreciated. Thus, the Al_2O_3 layer exhibits good durability and seems to be suitable for outdoor applications.

Similarly, samples A and B (Figure 4b,c, respectively) show a very similar surface morphology, free from defects. Despite the high humidity they were subjected to, the two composite layers still exhibit unchanged amounts of silver, as evidenced by EDXS analysis. Therefore, the test did not cause particular degradation of the silver particles. This result confirms a behavior observed in a previous work by Chen et al.,[45] which demonstrated the high thermal stability of Ag nanoparticles in anodized aluminum layers. At the same time, silver does not represent a defect in the composite layer, as it did not exacerbate the degradation of the alumina matrix during exposure in the climatic chamber. Ultimately, silver does not compromise the use of composite layers in outdoor environments subject to severe temperature changes.

3.2.2. Exposure to UV-B Radiation. To be employed in public places, these types of coatings must be able to withstand exposure to ultraviolet radiation. Therefore, the three series of samples were characterized by UV-B chamber tests, studying the possible degradation of silver. While aluminum oxide does not suffer from prolonged exposure to solar radiation, recent works demonstrated that UV light significantly enhances retention, dissolution, and oxidative aging of silver,[46,47] especially when subjected in synergy to high temperatures.[48]

The samples were exposed for 7 days to UV-B radiation at 50 °C, evaluating the change in morphology of the layers and silver amount. The images in Figure 5 show the surface of the

https://doi.org/10.1021/acsomega.2c02872
ACS Omega XXXX, XXX, XXX−XXX

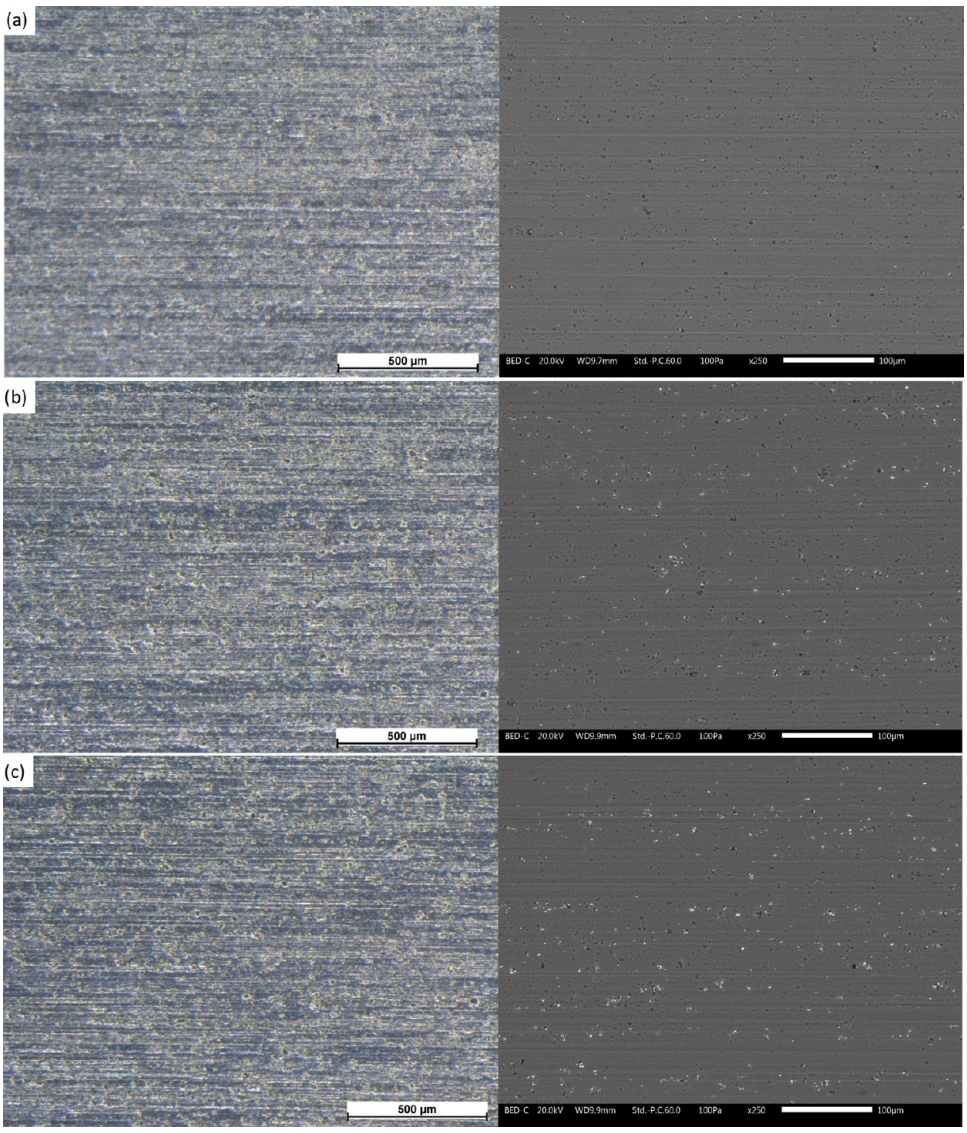

Figure 5. Micrographs of the surface of sample X (a), sample A (b), and sample B (c), respectively, after 7 days of exposure to UV-B radiation. The images on the left were collected by the optical microscope, while the corresponding ones on the right were acquired by the SEM.

three types of coatings at the end of the exposure, observed both by optical and electron microscopies, respectively, on the left and right of the images.

Macroscopically, none of the layers evidenced appreciable defects. Even by optical microscopy, it was not possible to highlight differences between the three samples. Similarly, SEM observations showed a morphology of the coatings unchanged over time: the layer of Al_2O_3 does not suffer from UV-B exposure and is not affected by the introduction of silver. However, as highlighted in the literature,[48] the synergy between high temperature and UV radiation caused the dissolution of silver. Table 2 shows the change in silver detected following exposure to the UV-B chamber. Although silver does not cause defects in the alumina layer, it suffers exposure to UV-B radiation, with consequent silver mass loss highlighted by SEM-EDXS analysis.

Consequently, the Al_2O_3−Ag composite layers, while showing high resistance to thermal changes, tend to lose the multifunctional features of silver when exposed to UV radiation. Therefore, the significant reduction of silver, after 7 days of testing in UV-B chamber, recommends avoiding the use of this type of material in direct contact with sunlight. However, the exposure to UV-B radiation represents a particularly aggressive test, not fully simulating the exposure to sunlight, in terms of frequency and intensity of the radiation. Ultimately, the test results do not represent a limit for the use of Al_2O_3−Ag layers in public environments, whose use can be intended for closed rooms, partially shaded spaces, or locations carefully protected from continuous solar radiation.

3.2.3. Kesternich Test. Figure 6 shows the surface appearance of the three series of samples after 7 days of the Kesternich test. The images evidence some differences between the three layers. In Figure 6b (sample A) and especially in Figure 6c (sample B), some defects are highlighted by red circles.

This test highlights the negative effect introduced by silver, which favors the development of defects during the exposure of the composite layers in the Kesternich chamber. The number of macroscopic defects arises with the increase in silver concentration. However, the coarse defects highlighted by the red circles are often accompanied by smaller defects, as shown in Figure 7. The image reveals a corrosion product larger than

https://doi.org/10.1021/acsomega.2c02872
ACS Omega XXXX, XXX, XXX−XXX

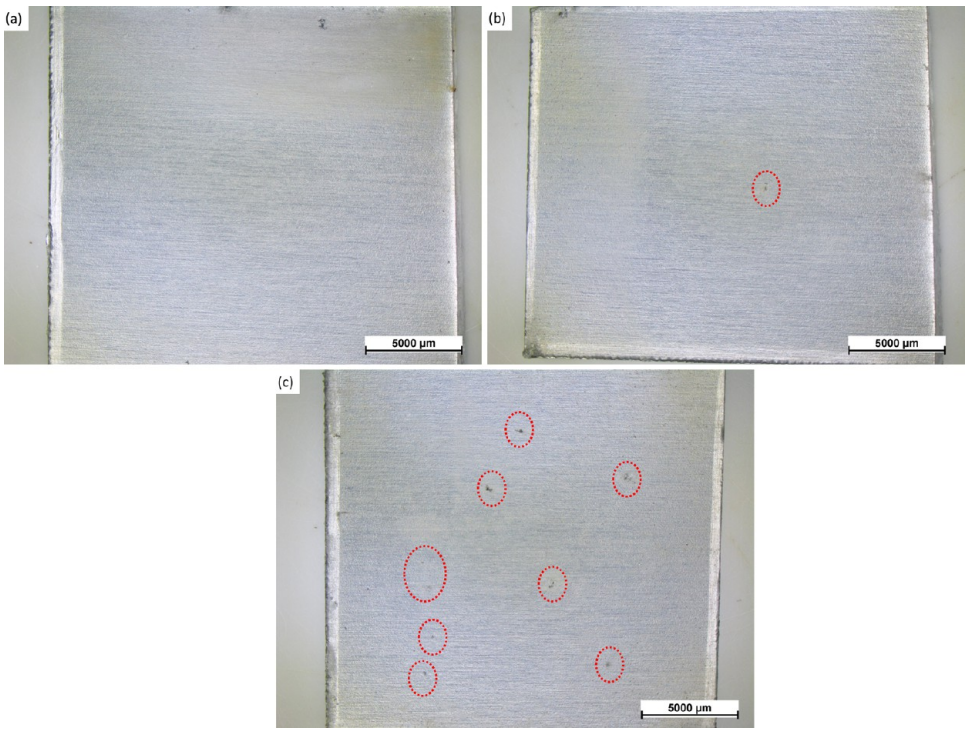

Figure 6. Optical micrographs of the surface of sample X (a), sample A (b), and sample B (c), respectively, after 7 days of the Kesternich test. The dashed circles highlight macroscopic defects.

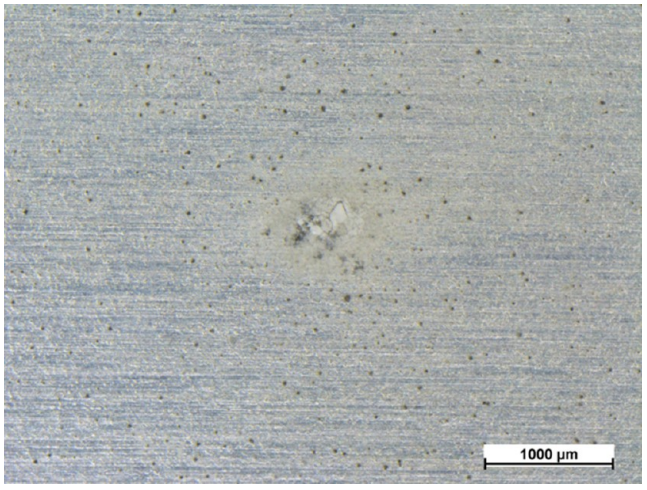

Figure 7. Optical micrograph of sample B with macro- and microdefects.

500 μm, surrounded by a multitude of black dots. These dark spots represent one of the most common defects in samples A and B following the Kesternich test. In fact, silver, in contact with the sulfur dioxide developed in the Kestenich chamber, reacts to form silver sulfide,[49−51] resulting in a dark appearance.

To study the evolution of this defect, the samples were monitored after 1, 3, and 7 days of exposure in the Kesternich chamber, analyzing them by SEM. Figure 8 reveals the different development steps of these silver sulfides on sample B. Figure 8a, acquired after 1 day of testing, shows a crystalline dendritic structure, typical of silver sulfides,[52] observed on the surface of the composite layer. This phenomenon occurs because the silver traces on the surface react quickly with the sulfur dioxide atmosphere. However, the prolonged contact with the aggressive atmosphere causes a growth of these products, whose dendritic morphology is further stressed.[53,54] The volumetric growth of the silver sulfate consequently causes the breakdown of the alumina layer, especially if it develops within the Al_2O_3 matrix. This phenomenon is represented by Figure 8b, observed after 3 days of permanence of the sample in the Kesternich chamber. The defectiveness of this stage constitutes the dark spots exhibited in Figure 7. Finally, after 7 days of exposure to the sulfur dioxide atmosphere (Figure 8c), the continuous volumetric growth of the silver sulfate causes severe degradation of the underlying aluminum alloy, resulting in large corrosion products. These corrosion outcomes are representative of the macroscopic defects highlighted by the red circles in Figure 6.

Ultimately, the high sensitivity of silver in atmospheres rich in sulfur precludes the use of this type of material in particularly aggressive environments such as industrial areas. Despite the good durability of aluminum oxide, the presence of silver represents a source of defects that cause accelerated degradation of the composite layer.

3.2.4. Silver Ions Release in Synthetic Sweat. A previous work of literature[37] has highlighted the strong degradation that alumina undergoes in contact with solutions simulating human sweat with particularly acidic pH. This phenomenon involves the release of silver present in the alumina layer, which could cause negative toxicological effects on human health.[55−59] As a matter of fact, silver intoxication (argyria) can happen through not only oral[60,61] but also dermal exposure.[62] Most of the silver risk assessments are related to argyria development: the World Health Organization (WHO) established a No Observable Adverse Effect Level (NOAEL) of 6.5 μg/kg body weight/day (bw/d),[63] while the US Environmental Protection Agency (US EPA) has given a reference dose (RfD) equal to 5 μg/kg bw/d

https://doi.org/10.1021/acsomega.2c02872
ACS Omega XXXX, XXX, XXX−XXX

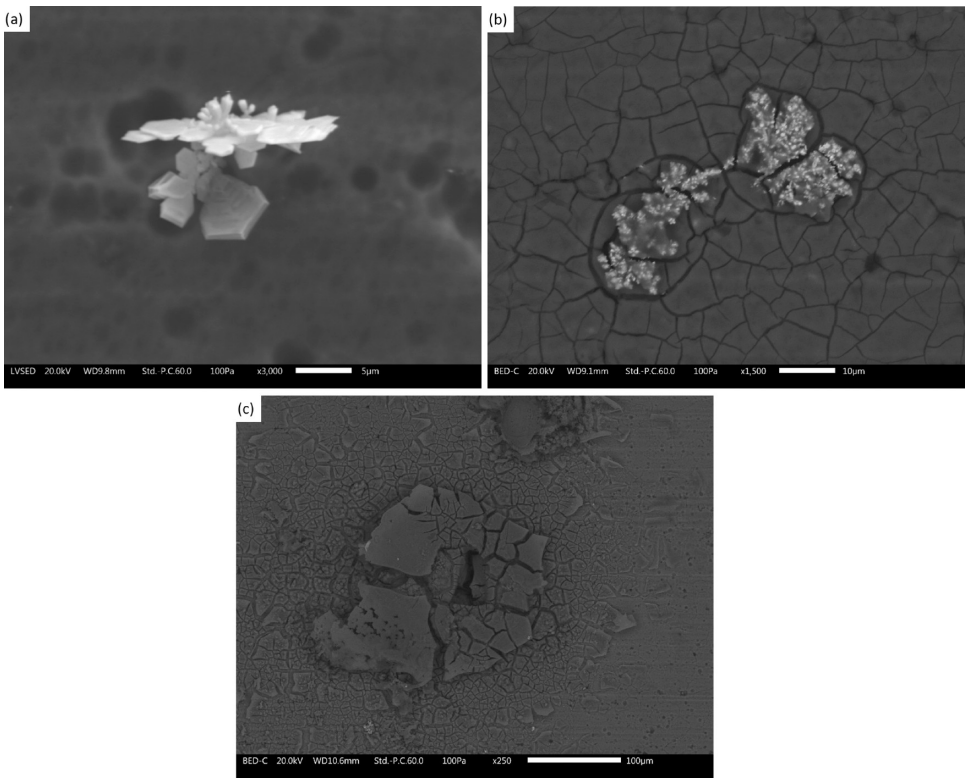

Figure 8. SEM micrographs of the surface of sample B after 1 day (a), 3 days (b), and 7 days (c) of the Kesternich test, respectively.

for chronic oral silver exposure,[64] corresponding to a total daily amount of 350 μg of silver for a 70 kg adult. Otherwise, the European Chemicals Agency (ECHA) has set even stricter limits, equal to 1.2 μg/kg daily, corresponding to 84 μg of silver for a 70 kg adult.[63]

Consequently, prolonged skin contact with Al_2O_3−Ag surfaces could cause undesirable effects on human health. Therefore, the release of Ag ions from samples A and B was evaluated by ICP analysis. To simulate the prolonged contact of the composite layers with human skin, the two series of samples were immersed in a 50 g/L lactic acid solution (pH = 2.1) at a temperature of 60 °C, modifying the perspiration test standard.[43]

The Ag ionic release values were monitored over time, up to a maximum of 28 days, as shown in Figure 9. Sample A and sample B exhibit a comparable behavior: a real increase in the concentration of silver present in the composite layer does not correspond to an appreciable difference in ion release examined by the ICP equipment.

However, the graph highlights that much of the release of Ag ions occurs during the first 6 h at values very close to the plateau reached after only 24 h of immersion in the test solution. The value of this plateau settles at about 0.7−0.8 μg/cm^2. Assuming that the contact between the human hand and the anodized aluminum component occurs on a surface of about 120 cm^2, the samples could release about 80−100 μg of silver in 24 h of continuous contact. These values largely fall within the limits imposed by the US EPA,[64] but they are also in line with the stricter limits recommended by the ECHA.[63] However, the test was carried out in a particularly aggressive environment. The contact conditions between the human skin and the surface of the composite layer were stressed by applying a high temperature, equal to 60 °C, in a particularly acid pH solution. Therefore, the test does not fully simulate

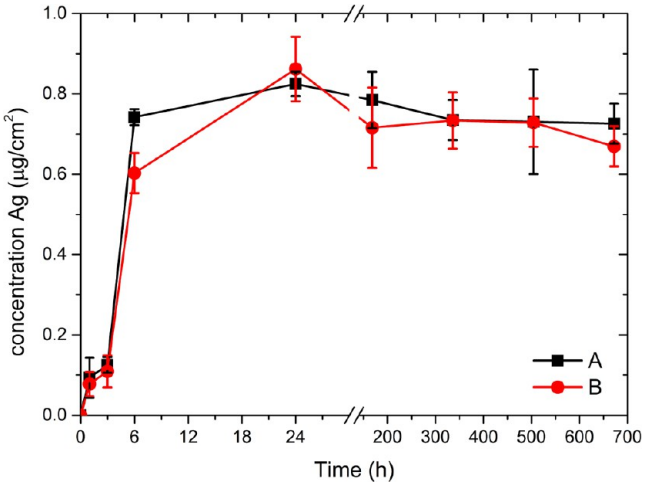

Figure 9. Ag ions release in synthetic sweat over time.

the direct contact between the human skin and the anodized aluminum surface, but rather accelerates these phenomena, offering largely precautionary and reassuring results in terms of low silver release by the two series of composite layers.

Furthermore, 0.8 μg/cm^2 represents the maximum amount of silver released during the whole test. After 24 h, therefore, the samples seem to lose all of the silver present inside the alumina matrix. This phenomenon is represented and explained in Figure 10, acquired by SEM.

Figure 10a shows the surface of sample A, observed after 6 hours of immersion in the test solution. Together with the silver deposited in cavities larger than 5 μm (white traces), the composite layer reveals the presence of numerous microcavities, with size less than 1 μm. These microcavities are due to the contact of the alumina-based layer with the lactic acid

https://doi.org/10.1021/acsomega.2c02872
ACS Omega XXXX, XXX, XXX−XXX

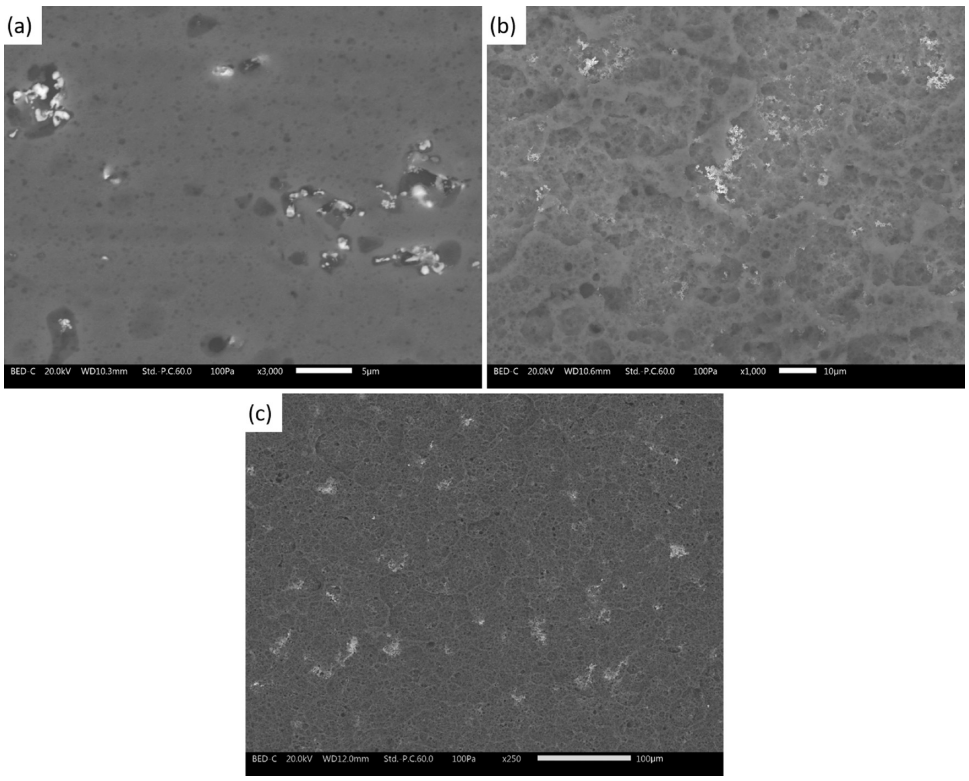

Figure 10. SEM micrographs of the surface of sample A after 6 h (a), 7 days (b), and 28 days (c) of the silver ion release test.

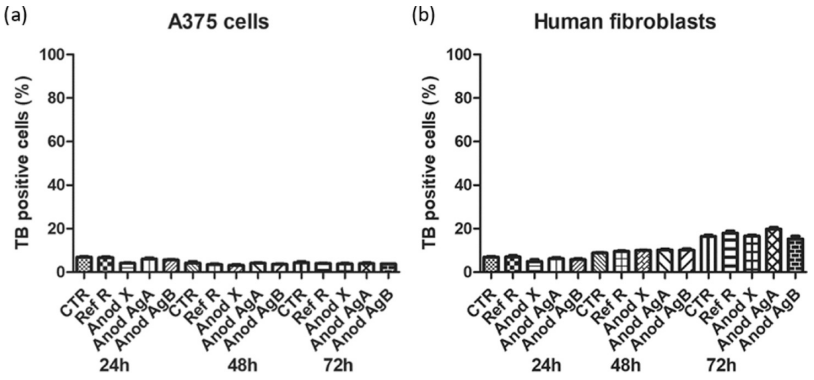

Figure 11. (a) Trypan blue results of A375 cell viability for 24, 48, and 72 h treated with aluminum (Ref R), anodized aluminum (Anod X), anodized aluminum with low silver concentration (Anod AgA), and aluminum anodized with high silver concentration (Anod AgB) showed no decreased cell viability comparison with control cells. (b) In human fibroblast cells, the lack of toxicity was revealed. The data and error bars represent the mean and SD of three independent experiments.

solution at a particularly acidic pH. As a matter of fact, the dissolution of the alumina layer in an acid environment has been extensively studied in the literature, and the poor durability of this material in similar solutions has already been highlighted in a previous work.[37] The first signs of dissolution of the alumina matrix inevitably cause the release of a large part of the silver inside it. However, as shown in Figure 10a, traces of silver can still be appreciated in the cavities of the composite layer. Otherwise, the morphology of the composite layer after 7 days of immersion is completely changed, as revealed in Figure 10b. The phenomenon of dissolution of aluminum oxide is at an advanced stage, and it is no longer possible to recognize the presence of a compact and continuous layer on the surface of the sample. In fact, EDXS analyses were not able to highlight an appreciable presence of silver: the white traces featured in the figure represent the presence of copper, an element contained in the 6082 aluminum alloy. Thus, the signal of copper suggests that the prolonged immersion in acid solution resulted in the almost complete removal of the composite layer, revealing the substrate of the 6082 aluminum alloy. This occurrence is further emphasized in Figure 10c, acquired at a low magnification at the end of the test: the Al_2O_3−Ag layer has been completely degraded by the long exposure to the test solution, and only the presence of copper can be appreciated as a representative of the metal substrate.

Thus, the images acquired by SEM explain the result obtained from the ICP analyses: the sudden release of silver ions is due to the rapid dissolution of the composite layer in contact with the acid solution. Although a plateau is reached in a short time, the quantity of silver analyzed complies with the limits required by the various European and American agencies, and it is associated with rapid degradation of the

https://doi.org/10.1021/acsomega.2c02872
ACS Omega XXXX, XXX, XXX−XXX

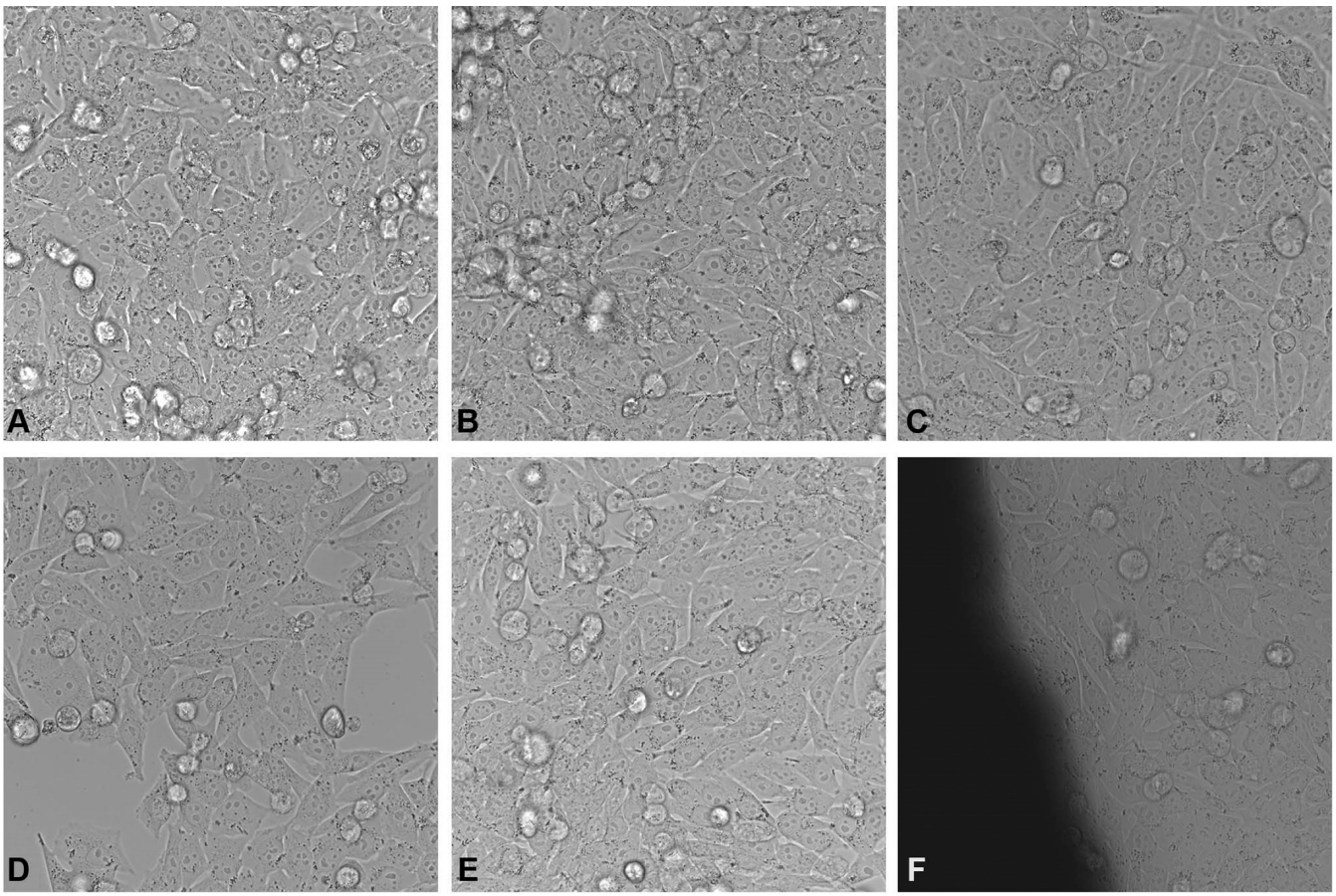

Figure 12. Optical microscopy observations of A375 control cells (A), after interaction with aluminum (B), anodized aluminium—sample X (C), anodized aluminum with low silver concentration—sample A (D), and aluminum anodized with high silver concentration—sample B (E, F). Magnification 1000×.

alumina matrix. In addition, the particular critical conditions under which the test was carried out must be considered. Ultimately, this type of sample does not present particular criticalities from the point of view of the release of Ag ions, suggesting its use in public environments, in continuous contact with human skin.

3.3. Cytotoxycity of Ag−Al_2O_3 Samples. *3.3.1. Viability of Melanoma Cells (A375) and Human Fibroblasts of Silver Anodized Aluminum Samples.* The cytotoxicity of the silver anodized aluminum samples was verified by Trypan blue flow cytometry analysis. The obtained results are shown in Figure 11a, where the viability of A375 cells remained above 90% on the third day of culture. Figure 11b quantifies the cell viability of human fibroblasts of a patient: at 72 h of compresence with anodized aluminum, the cell viability is about 80%. The cell viability of the control is, however, equal to the viability of cells with anodized aluminum and silver at higher concentrations (sample B). The 20% reduction in fibroblast cell viability can be attributed to a normal reduction due to cellular aging and nutrient deficiency.

3.3.2. Light Microscopy Observation of Nanomaterial Interactions with Human Melanoma or Fibroblast Cells. After assessing cell viability up to 72 h of immersion with the nanomaterial samples, the absence of cytotoxicity was confirmed by observation under a phase-contrast microscope. Figure 12 shows optical microscopy photographs of human melanoma cells added to the samples.

Observations were performed after 24, 48, and 72 h. Only the results acquired after 72 h are shown in Figure 12 for brevity. As can be seen, no obvious morphological changes are observed in any of the samples of treated human melanoma cells with sample A and sample B (Figure 12D,E), compared with control (Figure 12A), aluminum (Figure 12B), and anodized aluminum (Figure 12C). The cells are well adherent to the substrate, and their cell bodies are compact with no obvious signs of cellular distress. In the cellular population, there are numerous rounding indicating signs of cell division and therefore well-being of the population itself despite the presence of silver anodized aluminum. Figure 12F shows the reflected shadow of the silver anodized aluminum plate. The melanoma cells grew in a regular way even close to the metal structure, indicating that no mechanical perturbing effect or ionic release was detected by the cells.

Figure 13 reveals human fibroblast cells derived from a patient explant seeded on a plate of aluminum (Ref R), anodized aluminum (sample X), anodized aluminum with low contraction silver (sample A), and aluminum anodized with high contraction silver (sample B). The experiments were performed for 24, 48, and 72 h, but Figure 13 exhibits only the results acquired after 72 h. No morphological changes (Figure 13B−E) were observed even after the prolonged time (72 h) compared to the control (Figure 13A). Fibroblast cells grew normally even close to the plaque (Figure 13F), indicating that no hypothesis of damage was revealed.

https://doi.org/10.1021/acsomega.2c02872
ACS Omega XXXX, XXX, XXX−XXX

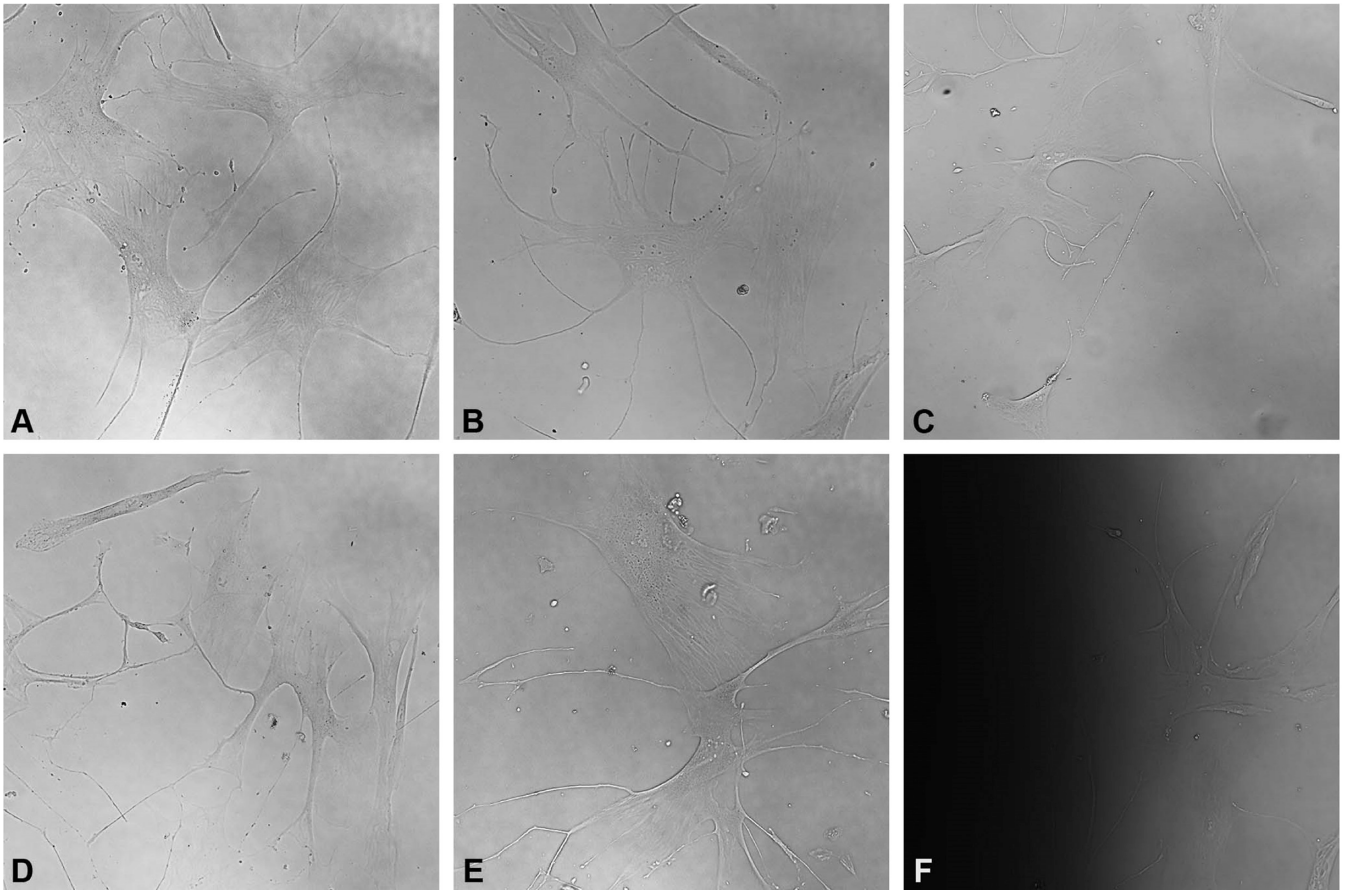

Figure 13. Optical microscopy observations of untreated human fibroblasts (A), after cells interaction with aluminum (B), anodized aluminium—sample X (C), anodized aluminum with low silver concentration—sample A (D), and aluminum anodized with high silver concentration—sample B (E, F). Magnification 1000×.

Ionic release of silver was also assessed by analyzing the culture media in which the two cell lines were maintained in growth simultaneously with the anodized aluminum samples with and without silver at two different concentrations. The analysis revealed no ionic release until 72 h of treatment (data not shown). These results support the cytotoxicity data obtained by cytofluorimetry (Figure 11). The data show that this type of material along with silver, known to be an element with antibacterial and antiviral properties, is compatible with surfaces that may be stressed by daily use.

4. CONCLUSIONS

This work aims to assess the durability of Al_2O_3−Ag composite layers, realized by a simple codeposition process, in different aggressive environments, with particular thermal changes, UV radiation, and sulfur dioxide atmosphere, evaluating the functionality of these materials in public spaces. With this in mind, the effect of silver on the cytotoxicity levels of the composite material was also studied to ensure its safe use in environments highly frequented by people.

Electron microscopy analyses highlighted that the addition of silver nitrate did not affect the yield of the anodizing process, obtaining consistent and defect-free composite layers. The codeposition process allowed the silver to deposit homogeneously on the surface of the samples and inside the alumina matrix in the proximity of magnesium and silicon traces.

The exposure of the samples in particularly aggressive atmospheres emphasized the high durability of the composite layer, whose performances were not negatively influenced by the silver additive. The Al_2O_3−Ag layers exhibited good resistance to thermal changes, simulated by a climatic chamber, as well as they revealed a good behavior when exposed to solar radiation. The only real limit to the use of these materials in public environments is represented by the high reactivity of silver in the presence of atmospheres rich in sulfur compounds, which cause tarnishing phenomena and consequent corrosion of the aluminum alloy, as observed following the Kesternich test. However, excluding "industrial" environments with a high rate of sulfides, this type of composite layer has proven to be suitable for outdoor applications.

Furthermore, to verify the safe use of these materials in close contact with human skin, ICP analyses of silver ion release were carried out, exposing the samples to an acid solution inspired by human sweat. The test, despite being particularly aggressive, showed a release of Ag by the samples that respects the limits imposed by the European and American agencies. The phenomenon of silver loss was studied by monitoring the samples through electron microscopy observations: the Ag release process is mainly due to dissolution processes of the alumina matrix in acid solutions.

Finally, the cytotoxicity of the Ag−Al_2O_3 samples was evaluated by cytometry analysis and optical microscopy observations. The tests evidenced no variations of cell viability

https://doi.org/10.1021/acsomega.2c02872
ACS Omega XXXX, XXX, XXX−XXX

due to the presence of silver, whose absence of cytotoxicity was confirmed by observation under a phase-contrast microscope.

Ultimately, this work introduces a simple and effective method for the implementation of silver into anodized aluminum layers, whose excellent durability performance, combined with the absence of cytotoxicity activity, makes it an excellent candidate for applications in public spaces.Table 3

Table 3. Silver Amount Detected Before and After the Sample Exposure to UV-B Radiation

sample	silver amount—day 0 [wt %]	silver amount—day 7 [wt %]
A	0.58 ± 0.06	0.41 ± 0.09
B	1.15 ± 0.07	0.68 ± 0.12

AUTHOR INFORMATION

Corresponding Author

Massimo Calovi − *Department of Industrial Engineering, University of Trento, Trento 38123, Italy;* orcid.org/0000-0001-6179-4842; Phone: +39-0461-282403; Email: massimo.calovi@unitn.it

Authors

Stefania Meschini − *National Center for Drug Research and Evaluation, National Institute of Health, Rome 00161, Italy;* orcid.org/0000-0001-9079-1181

Maria Condello − *National Center for Drug Research and Evaluation, National Institute of Health, Rome 00161, Italy*

Stefano Rossi − *Department of Industrial Engineering, University of Trento, Trento 38123, Italy*

Complete contact information is available at: https://pubs.acs.org/10.1021/acsomega.2c02872

Notes

The authors declare no competing financial interest.

ACKNOWLEDGMENTS

This research was funded by the RIVID project granted by the University of Trento in 2020 in the context of "Covid19" call.

REFERENCES

(1) Camargo, S. E. A.; Xia, X.; Fares, C.; Ren, F.; Hsu, S. M.; Budei, D.; Aravindraja, C.; Kesavalu, L.; Esquivel-Upshaw, J. F. Nano-structured Surfaces to Promote Osteoblast Proliferation and Minimize Bacterial Adhesion on Titanium. *Materials* **2021**, *14*, No. 4357.

(2) Otter, J. A.; French, G. L. Bacterial contamination on touch surfaces in the public transport system and in public areas of a hospital in London. *Lett. Appl. Microbiol.* **2009**, *49*, 803−805.

(3) Rai, N. K.; Ashok, A.; Akondi, B. R. Consequences of chemical impact of disinfectants: safe preventive measures against COVID-19. *Crit. Rev. Toxicol.* **2020**, *50*, 513−520.

(4) Scamans, G. M.; Birbilis, N.; Buchheit, R. G. Corrosion of aluminum and its alloys. In Shreir's. In *Corrosion*; 1st ed.; Elsevier: Amsterdam, 2010; pp 1974−2010.

(5) Furuya, S. Recent Trends and Development on Aluminum Surface Finishing Technology for Architecture. *Zairyo-to-Kankyo* **2001**, *50*, 94−97.

(6) Dyvik, S. H.; Manum, B.; Mork, J. H.; Luczkowski, M. Structural aluminum in architecture − the history and future of aluminum as a structural material. In *Structures and Architecture: Bridging the Gap and Crossing Borders*; 1st ed.; Cruz, P. J. S., Ed.; CRC Press: Boca Raton, 2019; pp 843−844.

(7) Liang, W. J.; Rometsch, P. A.; Cao, L. F.; Birbilis, N. General aspects related to the corrosion of 6xxx series aluminum alloys: exploring the influence of Mg/Si ratio and Cu. *Corrosion Sci.* **2013**, *76*, 119−128.

(8) Larsen, M. H.; Walmsley, J. C.; Lunder, O.; Mathiesen, R. H.; Nisancioglu, K. Intergranular corrosion of copper-containing AA6xxx AlMgSi aluminum alloys. *J. Electrochem. Soc.* **2008**, *155*, No. C550.

(9) Liu, X. Z.; Yang, J. H.; Wang, G.; Song, L. L.; Zhuang, G. S. Effect of Preparation Conditions on the Performance of Anodic Aluminum Oxide Films. In Applied Mechanics and Materials 1st ed.; Zhang, H.; Jin, D., Eds.; Trans Tech Publications Ltd.: Freienbach, 2012; pp 223−226.

(10) Rahimi, S.; Khiabani, A. B.; Yarmand, B.; Kolahi, A. Comparison of corrosion and antibacterial properties of Al alloy treated by plasma electrolytic oxidation and anodizing methods. *Mater. Today: Proc.* **2018**, *5*, 15667−15676.

(11) Liu, S.; Tian, J.; Zhang, W. Fabrication and application of nanoporous anodic aluminum oxide: A review. *Nanotechnology* **2021**, *32*, No. 222001.

(12) Lee, W.; Ji, R.; Gösele, U.; Nielsch, K. Fast fabrication of long-range ordered porous alumina membranes by hard anodization. *Nat. Mater.* **2006**, *5*, 741−747.

(13) Lee, W.; Park, S. J. Porous anodic aluminum oxide: anodization and templated synthesis of functional nanostructures. *Chem. Rev.* **2014**, *114*, 7487−7556.

(14) Habib, K. AC impedance−emission spectroscopy for determining the electrochemical behaviour of anodized aluminum in aqueous solution. *Nondestr. Test. Eval.* **2010**, *25*, 181−188.

(15) Hou, J.; Chung, D. L. Corrosion protection of aluminum-matrix aluminum nitride and silicon carbide composites by anodization. *J. Mater. Sci.* **1997**, *32*, 3113−3121.

(16) Li, S. M.; Li, B.; Liu, J. H.; Yu, M. Corrosion Resistance of Superhydrophobic Film on Aluminum Alloy Surface Fabricated by Chemical Etching and Anodization. *Chinese J. Inorg. Chem.* **2012**, *28*, 1755−1762.

(17) Zulaida, Y. M.; Ramadhanisa, A. H.; Partuti, T. The Effect of Electrolyte Concentration and Electric Current on the Quality of Surface Coloring on Anodized Aluminum. *Mater. Sci. Forum* **2020**, *988*, 42−47.

(18) Lee, C. C.; El-Zahlanieh, S.; Wang, Y. H.; Chen, C. C.; Chen, S. H.; Chang, Y. W. 6061 Aluminum Surface Treatment by High Quality Coloring Anodic Film. *Mater. Sci. Forum* **2020**, *975*, 31−36.

(19) Agbe, H.; Sarkar, D. K. Grant Chen, X. Electrochemically synthesized silver phosphate coating on anodized aluminum with superior antibacterial properties. *Surf. Coat. Technol.* **2021**, *428*, No. 127892.

(20) Jann, J.; Drevelle, O.; Grant Chen, X.; Auclair-Gilbert, M.; Soucy, G.; Faucheux, N.; Fortier, L. C. Rapid antibacterial activity of anodized aluminum-based materials impregnated with quaternary ammonium compounds for high-touch surfaces to limit transmission of pathogenic bacteria. *RSC Adv.* **2021**, *11*, 38172−38188.

(21) Agbe, H.; Sarkar, D. K.; Grant Chen, X.; Faucheux, N.; Souchy, G.; Bernier, J. L. Silver−Polymethylhydrosiloxane Nanocomposite Coating on Anodized Aluminum with Superhydrophobic and Antibacterial Properties. *ACS Appl. Bio Mater.* **2020**, *3*, 4062−4073.

(22) Russell, A.; Hugo, W. B. Antimicrobial activity and action of silver. *Prog. Med. Chem.* **1994**, *31*, 351−370.

(23) Baker, C.; Pradhan, A.; Pakstis, L.; Pochan, D. J.; Shah, S. I. Synthesis and antibacterial properties of silver nanoparticles. *J. Nanosci. Nanotechnol.* **2005**, *5*, 244−249.

(24) Morones, J. R.; Elechiguerra, J. L.; Camacho, A.; Holt, K.; Kouri, J. B.; Ramírez, J. T.; Yacaman, M. J. The bactericidal effect of silver nanoparticles. *Nanotechnology* **2005**, *16*, 2346−2353.

(25) Song, J. M. In *Silver as Antibacterial Agent: Metal Nanoparticles to Nanometallopharmaceuticals: (Silver Based Antibacterial Nano-metallopharmaceuticals)*, 2010 IEEE International Conference on Nano/Molecular Medicine and Engineering, IEEE, 2010; pp 98−101.

(26) Vithiya, K.; Kumar, R.; Sen, S. Antimicrobial activity of biosynthesized silver oxide nanoparticles. *J. Pure Appl. Microbiol.* **2014**, *4*, 3263−3268.

(27) Yin, I. X.; Zhang, J.; Zhao, I. S.; Mei, M. L.; Li, Q.; Chu, C. H. The antibacterial mechanism of silver nanoparticles and its application in dentistry. *Int. J. Nanomed.* **2020**, *15*, 2555−2562.
(28) Gonzalo-Juan, I.; Xie, F.; Becker, M.; Tulyaganov, D. U.; Ionescu, E.; Lauterbach, S.; De Angelis Rigotti, F.; Fischer, A.; Riedel, R. Synthesis of silver modified bioactive glassy materials with antibacterial properties via facile and low-temperature route. *Materials* **2020**, *13*, No. 5115.
(29) Dharmaraj, D.; Krishnamoorthy, M.; Rajendran, K.; Karuppiah, K.; Annamalai, J.; Durairaj, K. R.; Santhiyagu, P.; Ethiraj, K. Antibacterial and cytotoxicity activities of biosynthesized silver oxide (Ag_2O) nanoparticles using Bacillus paramycoides. *J. Drug Delivery Sci. Technol.* **2021**, *61*, No. 102111.
(30) da Silva, L. C. A.; Neto, F. G.; Pimentel, S. S. C.; da Silva Palácios, R.; Sato, F.; Retamiro, K. M.; Souza Fernandes, N.; Nakamura, C. V.; Pedrochi, F.; Steimacher, A. The role of Ag_2O on antibacterial and bioactive properties of borate glasses. *J. Non-Cryst. Solids* **2021**, *554*, No. 120611.
(31) Chi, G. J.; Yao, S. W.; Fan, J.; Zhang, W. G.; Wang, H. Z. Antibacterial activity of anodized aluminum with deposited silver. *Surf. Coat. Technol.* **2002**, *157*, 162−165.
(32) Tzaneva, B.; Karagyozov, T.; Dobreva, E.; Koteva, N.; Videkov, V. In *Conductive Silver Layers on Anodic Aluminum Oxide*, 2019 II International Conference on High Technology for Sustainable Development (HiTech), IEEE, 2019; pp 1−4.
(33) Pornnumpa, N.; Jariyaboon, M. Antibacterial and Corrosion Resistance Properties of Anodized AA6061 Aluminum Alloy. *Eng. J.* **2019**, *23*, 171−181.
(34) Ibrayev, N. K.; Aimukhanov, A. K.; Usupova, J. B. *Nanocomposite Material Based on Nanoporous Oxide of Aluminum with Additives of Silver and Gold Nanoparticles*, IOP Conference Series: Materials Science and Engineering, IOP Publishing, 2018.
(35) Sabry, R. S.; Ali Al-fouadi, A. H.; Habool, H. K. Enhanced antibacterial activity of anodic aluminum oxide membranes embedded with nano-silver-titanium dioxide. *J. Adhes. Sci. Technol.* **2018**, *32*, 874−888.
(36) Dehghan, F.; Mardanpour, H.; Kamali, S.; Alirezaei, S. Synthesis and antibacterial properties of novel Al_2O_3-Ag anodized composite coating. *Mater. Technol.* **2020**, *36*, 721−730.
(37) Calovi, M.; Furlan, B.; Coroneo, V.; Massidda, O.; Rossi, S. Facile route to effective antimicrobial aluminum oxide layer realized by co-deposition with silver nitrate. *Coatings* **2022**, *12*, No. 28.
(38) Mohamed, D. S.; El-Baky, A.; Sandle, T.; Mandour, S. A.; Ahmed, E. F. Antimicrobial Activity of Silver-Treated Bacteria against Other Multi-Drug Resistant Pathogens in Their Environment. *Antibiotics* **2020**, *9*, No. 181.
(39) Kaur, J.; Khatri, M.; Puri, S. Toxicological evaluation of metal oxide nanoparticles and mixed exposures at low doses using zebra fish and THP1 cell line. *Environ. Toxicol.* **2019**, *34*, 375−387.
(40) Chen, L.; Wu, M.; Jiang, S.; Zhang, Y.; Li, R.; Lu, Y.; Liu, L.; Wu, G.; Liu, Y.; Xie, L.; Xu, L. Skin Toxicity Assessment of Silver Nanoparticles in a 3D Epidermal Model Compared to 2D Keratinocytes. *Int. J. Nanomed.* **2019**, *14*, 9707−9719.
(41) ASTM G154-16, *Standard Practice for Operating Fluorescent Ultraviolet (UV) Lamp Apparatus for Exposure of Nonmetallic Materials*; ASTM International: West Conshohocken, PA, 2016.
(42) ASTM G87-02, *Standard Practice for Conducting Moist SO_2 Tests*, ASTM International: West Conshohocken, PA, 2002.
(43) ISO 12870:2016, *Ophthalmic Optics - Spectacle Frames - Requirements and Test Methods, 8.5 Test for Resistance to Perspiration*, ISO standards: London, UK, 2016, 1−19.
(44) Wang, X.; Santschi, C.; Martin, O. J. F. Strong Improvement of Long-Term Chemical and Thermal Stability of Plasmonic Silver Nanoantennas and Films. *Small* **2017**, *13*, No. 1700044.
(45) Chen, H.; Ohodnicki, P.; Baltrus, J. P.; Holcomb, G.; Tylcaz, J.; Du, H. High-temperature stability of silver nanoparticles geometrically confined in the nanoscale pore channels of anodized aluminum oxide for SERS in harsh environments. *RSC Adv.* **2016**, *6*, 86930−86937.
(46) Mittelman, A. M.; Fortner, J. D.; Pennell, K. D. Effects of ultraviolet light on silver nanoparticle mobility and dissolution. *Environ. Sci. Nano* **2015**, *2*, 683−691.
(47) Odzak, N.; Kistler, D.; Sigg, L. Influence of daylight on the fate of silver and zinc oxide nanoparticles in natural aquatic environments. *Environ. Pollut.* **2017**, *226*, 1−11.
(48) Lin, C. C.; Lin, D. X.; Lin, S. H. Degradation problem in silver nanowire transparent electrodes caused by ultraviolet exposure. *Nanotechnology* **2020**, *31*, No. 215705.
(49) Palomar, T.; Ramirez Barat, B.; Garcia, E.; Cano, E. A comparative study of cleaning methods for tarnished silver. *J. Cult. Herit.* **2016**, *17*, 20−26.
(50) Saleh, G.; Xu, C.; Sanvito, S. Silver tarnishing mechanism revealed by molecular dynamics simulations. *Angew. Chem.* **2019**, *131*, 6078−6082.
(51) Mao, X. Y.; Tian, K. S. Tarnish mechanism of silver plating and antitarnish process. *Electroplat. Pollut. Control.* **1995**, *15*, 8−12.
(52) Xie, S.; Zhang, X.; Xiao, D.; Paau, M. C.; Huang, J.; Choi, M. M. F. Fast growth synthesis of silver dendrite crystals assisted by sulfate ion and its application for surface-enhanced Raman scattering. *J. Phys. Chem. C* **2011**, *115*, 9943−9951.
(53) Valdez, B.; Schorr, M. *Environmental and Industrial Corrosion: Practical and Theoretical Aspects*; BoD−Books on Demand, 2012.
(54) Minzari, D.; Jellessen, M. S.; Moller, P.; Ambat, R. Morphological study of silver corrosion in highly aggressive sulfur environments. *Eng. Fail. Anal.* **2011**, *18*, 2126−2136.
(55) Lansdown, A. B. G. A pharmacological and toxicological profile of silver as an antimicrobial agent in medical devices. *Adv. Pharmacol. Sci.* **2010**, *2010*, 1−16.
(56) Reidy, B.; Haase, A.; Luch, A.; Dawson, K. A.; Lynch, I. Mechanisms of silver nanoparticle release, transformation and toxicity: a critical review of current knowledge and recommendations for future studies and application. *Materials* **2013**, *6*, 2295−2350.
(57) Lansdown, A. B. G. Silver in health care: antimicrobial effects and safety in use. *Curr. Probl. Dermatol.* **2006**, *33*, 17−34.
(58) Bouwmeester, H.; Dekkers, S.; Noordam, M. Y.; Hagens, W. I.; Bulder, A. S.; de Heer, C.; ten Voorde, S. E. C. G.; Wijnhoven, S. W. P.; Marvin, H. J. P.; Sips, A. J. A. M. Review of Health Safety Aspects of Nanotechnologies in Food Production. *Regul. Toxicol. Pharmacol.* **2009**, *53*, 52−62.
(59) Lead, J. R.; Batley, G. E.; Alvarez, P. J. J.; Croteau, M. N.; Handy, R. D.; McLaughlin, M. J.; Judy, J. D.; Schirmer, K. Nanomaterials in the Environment: Behavior, Fate, Bioavailability, and Effects-An Updated Review. *Environ. Toxicol. Chem.* **2018**, *37*, 2029−2063.
(60) Chang, A. L. S.; Khosravi, V.; Egbert, B. A Case of Argyria after Colloidal Silver Ingestion. *J. Cutan. Pathol.* **2006**, *33*, 809−811.
(61) Johnston, H. J.; Hutchison, G.; Christensen, F. M.; Peters, S.; Hankin, S.; Stone, V. A Review of the in Vivo and in Vitro Toxicity of Silver and Gold Particulates: Particle Attributes and Biological Mechanisms Responsible for the Observed Toxicity. *Crit. Rev. Toxicol.* **2010**, *40*, 328−346.
(62) Trop, M.; Novak, M.; Rodl, S.; Hellbom, B.; Kroell, W.; Goessler, W. Silver-Coated Dressing Acticoat Caused Raised Liver Enzymes and Argyria-like Symptoms in Burn Patient. *J. Trauma* **2006**, *60*, 648−652.
(63) SCENIHR (Scientific Committee on Emerging and Newly Identified Health Risks), Opinion on Nanosilver: Safety, Health and Environmental Effects and Role in Antimicrobial Resistance, European commission, 2014. https://ec.europa.eu/health/scientific_committees/emerging/docs/scenihr_o_039.pdf.
(64) U.S. Environmental Protection Agency Chemical Assessment, Silver CASRN 7440-22-4 jIRISjUS EPA, ORD, 1991. https://iris.epa.gov/ChemicalLanding/&substance_nmbr=99.

https://doi.org/10.1021/acsomega.2c02872
ACS Omega XXXX, XXX, XXX−XXX